



Modeling of Energy Stored by a Pumped Storage Power Plant using Wind Energy and Meteorological Data in Cameroon



Essoumam Nkanga Eddy Rodrigues^{1*}, Bissai Fontaine Dubois¹, Fouda Mbanga Bienvenu Gael², Toudna Abel³, Tekam Simeu Sylvère¹, Lontsi Frédéric¹

¹ National Higher Polytechnic School, University of Douala, 2701 Douala, Cameroon

² Department of Chemistry, Nelson Mandela University, 6031 Gqeberha, South Africa

³ Faculty of Science, University of Douala, 2701 Douala, Cameroon

* Correspondence: Essoumam Nkanga Eddy Rodrigues (edrod1717@gmail.com)

Received: 03-10-2025

Revised: 08-29-2025

Accepted: 09-25-2025

Citation: E. N. E. Rodrigues, B. F. Dubois, F. M. B. Gael, T. Abel, T. S. Sylvère, L. Frédéric, "Modeling of energy stored by a pumped storage power plant using wind energy and meteorological data in Cameroon," *Int. J. Energy Prod. Manag.*, vol. 10, no. 3, pp. 535–549, 2025. <https://doi.org/10.56578/ijepm100314>.



© 2025 by the author(s). Licensee Acadlore Publishing Services Limited, Hong Kong. This article can be downloaded for free, and reused and quoted with a citation of the original published version, under the CC BY 4.0 license.

Abstract: The particularity of renewable energy is its intermittency. One of the ways to make these sources exploitable is to propose efficient storage methods. This study develops a solution for storing wind energy, by gravity storage through water retention (wind-PSP system), and evaluates their effectiveness in the energy context of Cameroon. The methodology focuses on the use of wind energy to pump water to an upper basin. The methodological approach is based on mathematical and statistical modeling (water flows and wind distribution). These include the choice of study area using topographic data, digital terrain models applications and tools such as Google Earth, Global Positioning System (GPS), ArcGIS. The simulation model leads to an average available power of 12 MW for two water reservoirs with capacity of 95 m³ and 10 m³ whose heights are respectively 200 m and 2300 m above sea level. The field study contributes, with an experimental flow rate value of 4.42 m³/s, to support the site selection criterion due to the values in agreement with the literature. These results are encouraging and could be improved depending on the site.

Keywords: Gravity storage; Intermittency; Modeling; Renewable energies; Simulation; Wind-PSP system

1 Introduction

The global energy transition requires a drastic reduction in fossil fuels dependence in favor of renewable energy sources. These sources, although clean and abundant, exhibit variability and intermittency that complicates their massive integration into current electricity grids [1, 2]. In the absence of effective storage solutions, this variability harms the stability of the electricity system and limits the optimal use of these energies.

The Energy International Agency 2022 report states that the number of people living without electricity has increased for the first time in more than a decade. 685 million people did not have access to electricity in 2022, 10 million more than in 2021. Among them, 570 million live in sub-Saharan Africa, which thus concentrates more than 80% of the world's population without electricity [3]. The case of the Cameroonian energy system also experiences an imbalance between supply and demand, despite considerable hydraulic potential [4]. This alarming energy deficit (more than 40% of households do not have access to electricity in Cameroon [5]) could be attributed to the virtual non-existence of comprehensive studies to assess energy potential. This tool is essential and helps public authorities make decisions. We must also add the climate crisis, which is clearly the result of human activity [6–9].

Speaking of the climate crisis, the national report on climate and development published by the World Bank on November 5, 2022 deplores that climate change directly impacts more than 70% of the population whose livelihoods depend directly on agriculture. In recent years, Cameroon has made progress in developing climate plans and policy documents to integrate climate change into its sectoral strategies. The socio-economic impact of climate change shocks affects nearly 40% of vulnerable households. Over the past 20 years, the country has reduced its emissions through reforestation and by changing its energy mix in favor of renewable energy. This results in emissions reductions from 9.32 tonnes of carbon dioxide per capita in 1998 to 4.89 tonnes in 2018 [10].

In order to meet the ever-increasing demand for energy and at the same time meet the requirements of preserving

biodiversity, PSP-system seem adequate. The idea is to build a higher reservoir to store the water, and a lower one to receive this water which falls and must be reused several times [11, 12].

In the literature, only a few studies are conducted. Djongyang et al. [13] and Nouadje et al. [14] hypothetically assessed the wind potential in the Far North Region of Cameroon. In addition, Tchinda and Kaptouom [15] analyzed wind speeds and energy distributions in the Adamawa and Northern Regions of Cameroon. Nfah and Ngundam [16] identified stakeholders for sustainable growth of renewable energy in Cameroon. Arreyndip et al. [17] carry out a wind energy assessment of Cameroon's coastal regions for the installation of an onshore wind farm. Abanda [18] studied the potential, benefits, and enabling environment of renewable energy sources in Cameroon. Kaoga et al. [19] performed a statistical analysis of wind speed distribution using six Weibull methods to assess wind generation in the Northern Region. Kenfack-Sadem et al. [20] made up of the south, Littoral, central, west and south west potential of the wind energy in Cameroon based on weibull, normal and lognormal distribution. Kaoga et al. [21] assessed the potential of wind energy for water pumping at scale and concluded that the potential in the Northern Region of Cameroon is not suitable for electricity generation. Speaking of energy storage in the form of water, some studies have already been conducted in the context of domestic operation powered by solar panels ; in particular Pali and Vadhera [22] proposed system comprises of a solar photovoltaic (SPV) system, solar water pump, pico-hydro turbine-generator and pumped-hydro energy storage system. Olabi [23] proposed installation of an appropriately administered wind powered pumped hydro storage system with an hypothetic storage of 5,000,000 m³ of water and the turbine power of 20 MW.

However, gravity storage in the form of water retention of wind energy in seasonal mode is not developed in scientific research. To this end, a question deserves to be asked, that of knowing how to optimize the storage of wind energy in the energy context of Cameroon?

The aim of the work is to model a renewable energy storage solution (wind-PSP) and evaluate its efficiency in an energy system powered mainly by intermittent renewable sources such as wind power in the context of Cameroon.

The study is divided into three sections; the section entitled materials and methods is devoted to the presentation of the tools, software, data collected, and the description of the wind energy storage system chosen. The experimental method deployed for measuring the flow rate of the watercourse in the study area is developed to meet the topographical conditions. Section two focuses on the various simulation and experimental results of the proposed and developed energy storage system. A summary of a study is drawn up as a conclusion to the work, which ends with elements of perspectives.

2 Materials

Emphasis is placed on the use of specialized software and robust hardware to reduce computational time. Experimental flow measurement requires a procedure and tools. These are also presented in this section.

For this work, the software and hardware tools used are detailed as follows:

- **Matlab/Simulink**

This software is used in this article to create dynamic models of wind turbines. It integrates climate variations (wind speed) from measured or synthetic data. It simulates the PSP (pumped storage) system by modeling pumping, turbine, and water level management cycles. Broadly speaking, the Matlab/Simulink application is a tool for validating theoretical hypotheses through simulation [24–27].

- **Google Earth**

The Google Earth application enabled the selection of the potential PSP site location by identifying areas with good wind potential near terrain suitable for the creation of high-altitude reservoirs [28]. The application also enabled the evaluation of the elevation profile and the analysis of the available elevation difference between two points (essential for the efficiency of gravity storage).

- **ArcGIS 10.8**

ArcGIS software allows the creation of digital elevation model (DEM) to simulate the elevation differences between the upper and lower reservoirs [29–31]. It automatically calculates slope, orientation, and elevation to identify the most efficient locations in terms of gravitational potential. This application is useful in estimating the potential water retention volume based on topography.

- **GPS Garmin 64 s**

The Global Positioning System (GPS) tool is used in this work to locate the study area that may house production and storage sites [32]. This tool allows the precise identification of the geographical coordinates of the installations. It is used to study the wind potential of a site based on geographical and climatic data (wind, latitude, longitude, altitude, etc.) that can be used for the application of a wind- pumped storage power plant (wind-PSP).

- **Weather Data Collection Sheet**

The meteorological data collection sheet plays an essential role in the observation and analysis of climate and weather; allows for the systematic collection of meteorological data such as temperature, humidity, atmospheric

pressure, wind speed and direction [33, 34]. An important step in this article is obtaining meteorological data. This was obtained from the decentralized services of the Ministry of Transport, notably the Regional Delegation of the Coastal Region.

- **Tape Measure**

The tape measure is used to measure distances in the field (length, width, water surface, etc.). This instrument was used to measure the width of a riverbed (see float method) [35]; was also used to measure the longitudinal marker of the float's passage.

- **Stopwatch**

The stopwatch in this article is used to determine the time taken for the float to pass along the marker.

3 Methods

The storage solution modeling method made it possible to subdivide this work into five main parts: a description of the wind energy storage system, a mathematical modeling of the system components taking into account environmental conditions, a location of the study area suitable for the wind-PSP project, their simulation in the ArcGIS, Matlab/Simulink platforms and finally an experimental flow measurement in the study area.

3.1 Description of the Wind Energy Storage System: Gravity Storage by Water Retention (Wind-PSP)

The proposed system with pumped storage is shown in Figure 1. The main components of the system include a power generator (wind turbine), an energy storage subsystem (pumped storage with two reservoirs, pumps, and turbines/generators), a user (load), and a control station. The entire system is regulated by the control center, which is the critical element of the overall load management and power distribution system.

Diurnal and seasonal variations in wind direction and speed were taken into account with meteorological data that integrate favorable wind directions as well as minimum and maximum speeds reached in the measured region.

The strategies and control logic of the actual operation were not considered in this study because the scope of study was restricted to the evaluation of producible power due to the flow of water from one height to another at the turbine inlet. In addition, an assumption of water as a perfect fluid is made. Hence the control logic in this context cannot have a significant impact on the system

Three-blade wind turbines are the most used because they offer better regularity and better balance of the rotor [36]. Horizontal axis wind turbines can also be classified according to the direction of incidence of the wind. In this case, turbines upstream of the wind for which the wind hits the blades directly and turbines downstream of the wind for which the wind hits the back of the blades [37].

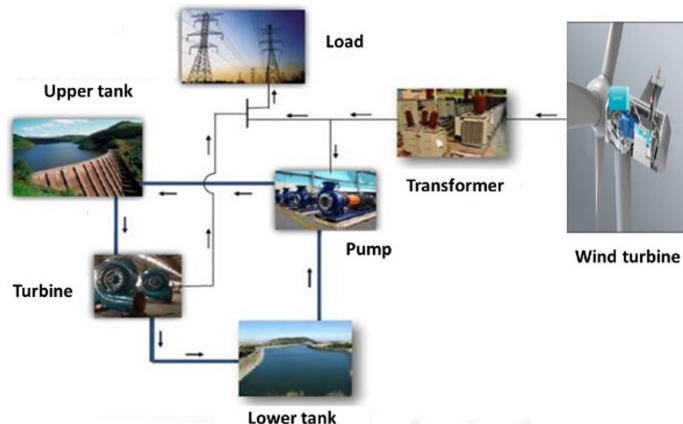


Figure 1. Closed-cycle wind energy gravity storage system (wind-PSP)

3.2 Location and Ddescription of a Study Area Favorable to the Wind-PSP Storage System

Pumped storage system modeling is dependent on meteorological data in our context, with the use of wind power to pump water. In this study, the available meteorological data are those of the coastal region shown in Figure 2. The topography of the coastal region suggests areas of steep slopes in the Moungou department as shown in the Figure 3. This is the reason that led to the study of the Nkongsamba site, which, with its elevation differences ranging from 200 m to 2300 m (see Figure 4), is a suitable area for a pumped storage system using wind power. The limitation in the choice of regions is mainly due to obtaining meteorological data.

The sustainable use of water resources in Cameroon in determining reservoir capacity and water flow in Cameroon begins with the description of the study area under the heading "Relief and Hydrography." This includes listing the main watershed, its tributaries, and the main rivers flowing from them.

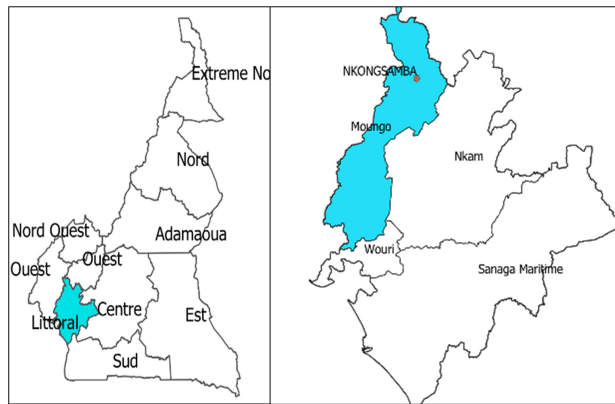


Figure 2. Location of the study area

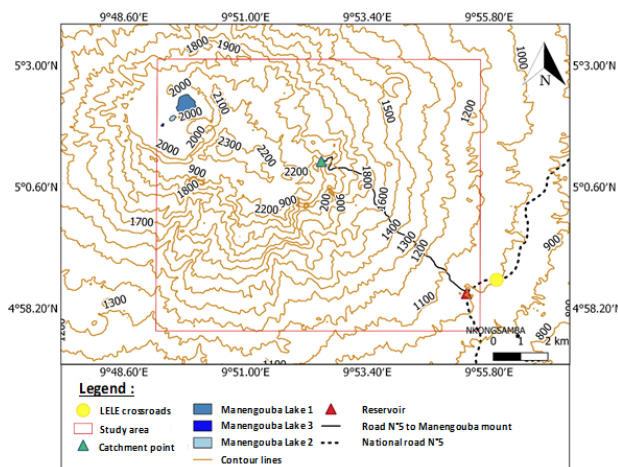


Figure 3. Topographic map of the study area

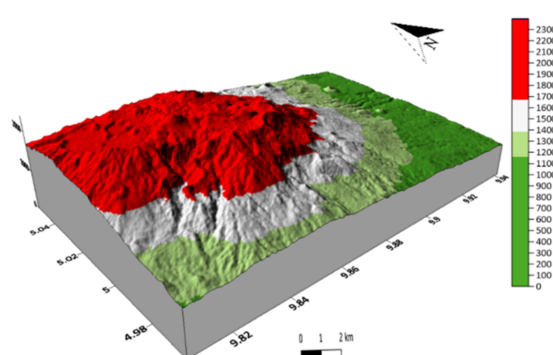


Figure 4. Digital terrain model of the study area

3.3 Modeling of the Components of Water-Retention Gravity Storage Systems: Conventional PSP and Wind-PSP

In the literature, two significant variables for the design of pumping systems are the volume of the upper reservoir and the height difference between the upper and lower reservoir [38]. Bernoulli's equation is one of the most useful equations that is applied in a wide variety of fluid flow problems. In a simple form, Bernoulli's equation relate pressures (P_1, P_2), velocities (V_1, V_2), and elevations (h_1, h_2) between any two points (1 and 2) in the flow field.

Bernoulli Equation with Losses

Since the piping system includes accessories (elbows, valves, etc.)

$$P_1 + \frac{1}{2} \cdot \rho v_1^2 + \rho g h_1 + \Delta h = P_2 + \frac{1}{2} \cdot \rho v_2^2 + \rho g h_2 + \Delta h \quad (1)$$

where, ρ is the density of water (1000 kg/m^3), g is the acceleration due to gravity (9.81 m/s^2) and Δh is the pressure, The output power of the hydroelectric turbine is totally dependent on the head h and the flow rate F available at the site, the fluid density ρ , the turbine efficiency η and the force of gravity g . The output power P is given by the Eq. (2):

$$P = \eta \rho F g h \quad (2)$$

Determining the Power Supply for Mechanical Storage

The redundant design is partially taken into account given the hypothesis of water as a perfect fluid. The reliability of the system is determined by the reliability of the elements that constitute the system. The non-implementation of a restricted experimental device restricts the reliability of the system to the study of the flow of water from one height to another while considering the other elements of the device without potential energy losses. Hence the system with the listed assumptions can operate continuously without interruption.

The required wind turbine power must be greater than the pump-turbine power to ensure the system operates properly ($P_{\text{turbine}} \geq P$).

First, the pump-turbine's hydraulic power must be determined based on its physical and technical characteristics. Then, knowing from Eq. (3) that

$$P = \eta \rho F g h \quad (3)$$

By determining the flow rate at a given height, the reservoir capacity can be deduced.

The determination of the wind turbine power can be carried out using the equation used Eqs. (4) and (5) [39]. To determine the wind turbine's power, the exact wind speed at the height of the wind turbine's rotor must be known. Wind speed is often measured at sea level or at special measuring facilities with a defined height of about 4 m, which is significantly lower than the height of a wind turbine. Therefore, the measured data must be corrected to the desired height using Eq. (4).

The wind speed V_{wind} at height z_{wind} can be determined from the measured wind speed $V_{\text{wind,ref}}$ at height $z_{\text{wind,ref}}$ (4 m) in combination with the terrain roughness z_0 .

$$V_{\text{wind}} = V_{\text{wind,ref}} \frac{\ln\left(\frac{z_{\text{wind}}}{z_0}\right)}{\ln\left(\frac{z_{\text{wind,ref}}}{z_0}\right)} \quad (4)$$

To obtain the output power of a wind turbine P_{turbine} , the theoretical wind power P_{wind} must first be calculated using Eq. (5). Therefore, the air density ρ_a (from 1.22 to 1.3 kg/m^3), the area covered by the rotor blades A , and the wind speed are required.

$$P_{\text{wind}} = 1/2 (\rho_a A v_{\text{wind}}^3) \quad (5)$$

The maximum wind power cannot be fully converted into wind energy. This circumstance is taken into account by applying the coefficient of performance C_P , which reduces the maximum achievable power. The actual power of the wind turbine results from the product of the wind power and the coefficient of performance as illustrated by the Eq. (6).

$$P_{\text{turbine}} = P_{\text{wind}} \cdot C_P \quad (6)$$

The coefficient of performance of conventional wind turbines is limited to $C_P = 0.593$ [40].

Wind Modeling

When using the Weibull distribution for wind speed modeling, the model assumptions were tested in the application of the Newton Raphson algorithm. The actual data exhibit a slight disparity due to the form factor which is high after determining the Weibull parameters. Hence the actual data are approximately consistent with the distribution assumptions with a negligible margin of error. However, to obtain a reliable assessment of the average speed and its variance at a given point, approximately ten years of measurements are required. Finding a method describing wind behavior based on a much shorter (annual) measurement period is advisable. Research able to establish that the most appropriate method is the two-parameter Weibull function [41].

Weibull Distribution

The choice of the Weibull model is justified by the literature because of its reliability for its two-parameter model.

In the Weibull distribution, wind speed variations are characterized by two functions: the probability density function and the distribution function.

$$f(v) = \frac{k}{c} \left(\frac{v}{c} \right)^{k-1} \exp \left[- \left(\frac{v}{c} \right)^k \right] \quad (7)$$

$$F(v) = \int_0^v f(v) dv = 1 - \exp \left[- \left(\frac{v}{c} \right)^k \right] \quad (8)$$

In the presented distribution model, the parameters shape factor k and scale factor λ are unknown and must be determined.

Analytical and Numerical Approach to Resolution

Definition: Let X be a random variable (V.a).

The V.a X is distributed according to a two-parameter Weibull distribution if there exist values (parameters) $C, \alpha (C, \alpha > 0)$ such that the V.a:

$$Y = \left(\frac{X}{\alpha} \right)^c \quad (9)$$

The Eq. (9) is distributed according to an exponential law with probability density function g , with

$$g(y) = e^{-y}, \text{ pour } y > 0. \quad (10)$$

and its distribution function is:

$$F(x) = 1 - \exp \left(\left(-\frac{x}{\alpha} \right)^c \right), x > 0. \quad (11)$$

Maximum Likelihood Estimation of the Parameters of a Weibull Distribution

Let X_1, X_2, \dots, X_n be n random variables with identically distributed intervals of the Weibull distribution with parameters (α, c) of density function f_i given by:

$$f_i(y) = \frac{c}{\alpha} \left(\frac{y}{\alpha} \right)^{c-1} \exp \left(\left(-\frac{y}{\alpha} \right)^c \right), y, \alpha, c > 0 \dots i = 1, \dots n. \quad (12)$$

The density function of the variable $X = \prod_{i=1}^n x_i$ denoted f is given for all $x = (x_1, x_2, \dots, x_n) \in X$ by:

$$f(x) = \prod_{i=1}^n f_i(x_i). \quad (13)$$

In the following we propose to estimate the parameters (α, c) of the Weibull law using the maximum likelihood principle. Let us denote by $L(\cdot, \cdot)$ the likelihood function of a realization x_1, x_2, \dots, x_n . We have for any pair (α, c) .

$$L(\alpha, c) = \prod_{i=1}^n f_i(x_i). \quad (14)$$

Taking the logarithm of Eq. (9) yields the log-likelihood function:

$$\ln(L(\alpha, c)) = n \ln(c) - n \ln(\alpha) - \sum_{i=1}^n \left(\frac{x_i}{\alpha} \right)^c + (C-1) \sum_{i=1}^n \ln \left(\frac{x_i}{\alpha} \right). \quad (15)$$

Determination of the Parameters of the Maximum Likelihood

In this part it is a question of finding the two parameters: the parameter of form \hat{c} and of scale $\hat{\alpha}$ which maximize the estimate. These parameters are obtained by solving the system

$$\begin{cases} \frac{\partial}{\partial \alpha} (\ln((L(\alpha, c))) = 0, \\ \frac{\partial}{\partial c} (\ln((L(\alpha, c))) = 0. \end{cases} \quad (16)$$

Taking into account that:

$$\frac{\partial}{\partial c} \left[e^{c \times \ln \left(\frac{x_i}{\alpha} \right)} \right] = \ln \left(\frac{x_i}{\alpha} \right) \left(\frac{x_i}{\alpha} \right)^c, \quad (17)$$

We then obtain:

$$\alpha = \left(\frac{1}{n} \sum_{i=1}^n x_i^c \right)^{1/c}. \quad (18)$$

Considering that,

$$\sum_{i=1}^n \ln \left(\frac{x_i}{\alpha} \right) \left(\frac{x_i}{\alpha} \right)^c = \sum_{i=1}^n [\ln(x_i) - \ln(\alpha)] \frac{x_i^c}{\alpha^c} = \sum_{i=1}^n \frac{x_i^c \ln x_i}{\alpha^c} - \sum_{i=1}^n \frac{x_i^c \ln(\alpha)}{\alpha^c} \quad (19)$$

It comes after some calculations;

$$\frac{n}{c} - \sum_{i=1}^n \frac{x_i^c \ln x_i}{\alpha^c} + \sum_{i=1}^n \ln(x_i) = 0. \quad (20)$$

Which finally gives,

$$c = \left[\left(\sum_{i=1}^n x_i^c \ln(x_i) \right) \left(\sum_{i=1}^n x_i^c \right)^{-1} - \frac{1}{n} \sum_{i=1}^n \ln(x_i) \right]^{-1}, \quad (21)$$

From where

$$\begin{cases} \hat{\alpha} = \left(\frac{1}{n} \sum_{i=1}^n x_i^c \right)^{\frac{1}{c}} \\ \hat{C} = \left[\left(\sum_{i=1}^n x_i^c \ln(x_i) \right) \left(\sum_{i=1}^n x_i^c \right)^{-1} - \frac{1}{n} \sum_{i=1}^n \ln(x_i) \right]^{-1} \end{cases} \quad (22)$$

Or even

$$\begin{cases} \hat{k} = \left(\frac{\sum_{i=1}^n x_i^k \log X_i}{\sum_{i=1}^n X_i^k} - \frac{1}{n} \sum_{i=1}^n \log X_i \right)^{-1} \\ \hat{\lambda} = \left(\frac{1}{n} \sum_{i=1}^n X_i^{\hat{k}} \right)^{\frac{1}{\hat{k}}} \end{cases}$$

In order to make Eq. (22) more usable and to facilitate its execution by the Newton Raphson algorithm, a detailed development was carried out (in particular the analytical determination of the derivative of the function) with some simplifying hypotheses.

Starting from the function:

$$g(c) = \frac{\sum_{i=1}^n x_i^c}{\sum_{i=1}^n x_i^c \ln(x_i) - \frac{1}{n} \sum_{i=1}^n x_i^c \sum_{i=1}^n \ln(x_i)}$$

And by applying the derivative member by member we obtain after simplifications

$$g'(c) = \frac{\sum_{i=1}^n c x_i^{c-1} \sum_{i=1}^n x_i^c \ln(x_i) - \frac{1}{n} \sum_{i=1}^n c x_i^{2c-1} \sum_{i=1}^n \ln(x_i) - \frac{1}{n} \sum_{i=1}^n x_i^{2c-1} ((\sum_{i=1}^n c \cdot \ln(x_i) + 1))}{(\sum_{i=1}^n x_i^c \ln(x_i) - \frac{1}{n} \sum_{i=1}^n x_i^c \sum_{i=1}^n \ln(x_i))^2} \quad (23)$$

where, n = number of non-zero data values; i = measurement interval; ν = wind speed measured at interval i ($m \cdot s$).

Numerical Method for Compiling the Wind Energy Storage Model in the Form of Gravity Water Retention

The meteorological data used in the study cover the period 2020–2023. These data were compiled as cumulative monthly averages over the four years and presented in Table. The sample size is sufficient, based on the extrapolation methods, to ensure the accuracy of the model. These data are up-to-date and available from local meteorological services.

A brief reading of the meteorological data obtained suggests daily data collection with a 6-hour time step for wind speed, sunshine, and direction. This indicates that seasonal and interannual variations in the data were taken into account, as these data incorporate them.

Wind turbine

Input parameters

$z_{windref} = 4$;

$V_{windref} = [3.060483871 \ 3.556451613 \ 3.286290323 \ 3.116935484 \ 3.14516129 \ 3.028225806 \ 3.036290323 \ 3.370967742 \ 3.040322581 \ 3.286290323 \ 3.463709677 \ 3.39516129]$;

$z_0 = 1$; $\rho = 1.22$; $A = 12.5$; $C_p = 0.5$.

3.4 Estimation of the Flow Rate of a Watercourse in the Study Area

The discharge was measured using the float method. This method requires a numbers of tools, which are described in Section 2. Figure 5 shows the watercourse, and some of the tools used for this measurement.



Figure 5. Watercourse study area

Regarding the float method used to measure river flow, irregularity is taken into account through the plurality (at least three) of flow velocity measurements. On the other hand, the influence of morphology is not taken into account by assuming the natural flow of water. The application of a correction coefficient is integrated into the float method to compensate for measurement uncertainties and errors. When the float passes the observer, the timer is started and stopped when it passes the marker downstream. At least three successive measurements should be taken. Therefore, the surface speed is:

$$V_s = \frac{\text{distance} \times 3}{\text{time 1} + \text{time 2} + \text{time 3}} \quad (24)$$

Since the current speed is faster at the surface, a correction factor of 0.6 is used to calculate the average speed from the surface speed:

$$V_m = V_s \times 0.6 \quad (25)$$

The river's width is measured by stretching a marked rope across the watercourse perpendicular to the current. As you cross the watercourse, you will note the average depth, which will be measured upon returning to the bank with a rigid tape measure.

Calculating the flow rate (F):

$$F = V_m \times l \times P_m \quad (26)$$

4 Results and Discussion

4.1 Weibull Adjustment and Wind Potential Estimation

In the context of gravitational storage of wind energy, it is crucial to have a good understanding of the temporal profile and variability of wind speed. This allows for the appropriate sizing of pumping and water retention infrastructure use in gravitational storage, this involves wind speed data collection and data extrapolation hourly or daily at the site under study, estimating the parameters k and c using the maximum likelihood method.

Weibull distribution fitting is a commonly used method to model wind speed distribution and estimate the wind potential of a site. Once the maximum likelihood estimators (MLEs) are found using the Newton Raphson algorithm (Eq. (23)) in MATLAB software, it is possible to plot the fitted Weibull distribution density curve in MATLAB over the frequency histogram. Figure 6 shows the fitting of a Weibull density function to the wind speed distribution in m/s.

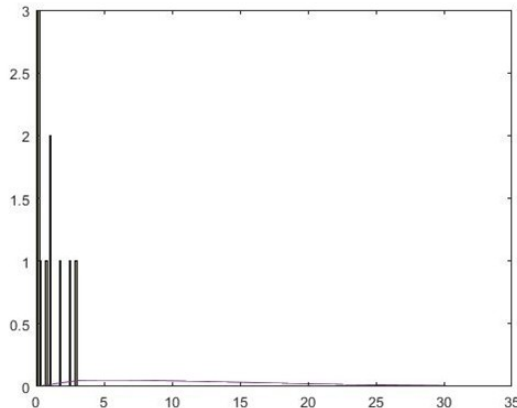


Figure 6. Weibull fit to the wind speed histogram

The curve describes on the one hand a histogram of wind speeds on the frequencies of occurrence. When observing this figure, we can note that at the level of the coast, i.e. for an altitude of 3 m maximum above sea level, the wind speeds are low; [0, 2] m/s with the highest frequencies of the order of 3. The higher we go in altitude, the more the speed increase as well as their frequency of occurrence.

On the other hand, the adjustment curve of the Weibull density function reveals 03 slopes. A first increasing slope for speeds ranging from [0, 5] m/s; this is an operation of the wind turbine with a low wind regime that cannot cause any major failure. A slightly constant slope for speeds ranging from [5, 15] m/s; this is a standard operating regime of the wind turbine. A third steep decrease slope ranging from 15 to 25 m/s; this is a critical operating regime for the wind turbine. Here, we can see that the speed cancel out for winds over 25 m/s; this is the phenomenon of dynamic stalling.

Comparison with the Literature

The two main parameters obtained by the site are compared with typical values in the literature as shown in Table 1. This comparison is based on the following comments:

Table 1. Prediction of whole year Weibull parameters by different methods

Weibull Method	Weibull Parameters		Kolmogorov-Smirnov Test			Statistical Tests		
	Scale C	Scale k	KOL _{0.10}	KOL*	KOL 0.1-KOL*	RMSE	R^2	χ^2
EM	2.1478	1.7115	0.7671	0.0663	0.0805	0.0570	0.7334	0.1917
EPF	2.1589	1.6245	0.7674	0.0485	0.1219	0.0699	0.7570	0.1467
GM	2.6682	1.6019	0.7690	0.0556	0.1905	0.0748	0.7924	0.2978
MLM	2.1595	1.7245	0.7680	0.0585	0.0805	0.0659	0.7469	0.1422
MDLM	2.1678	1.8114	0.7767	0.0740	0.0246	0.0600	0.7057	0.0927
MM	2.1453	1.6866	0.7627	0.0749	0.0923	0.0558	0.7403	0.1831

$k > 2$: steady winds (good for wind power);

$k < 1.5$: erratic winds;

The higher C , the more suitable the site is for wind power generation.

In the illustration, the comparison is made with the maximum likelihood method (MLM) as developed. The value of $k^\wedge = 1.37$ is similar to that obtained by Kaoga et al. [21], namely 1.7425, or a relative difference rate of -21.37%. This difference can be explained by the differences in weather conditions between the sites.

The value of $C^\wedge = 14.2326$ is significantly higher than that of Kaoga et al. [21], namely 2.1595. The relative difference rate is 84.83%. This difference can be explained by the differences in weather conditions between the sites and also by the difference in numerical simulation approach, which, in this article, is the Newton-Raphson algorithm and for the article by Kidmo and al., the modified maximum likelihood method.

4.2 Determination of the Available Power and Flow Rate of the Wind Storage-PSP System

The evaluation of the efficiency of the wind-PSP system in this study was restricted to the evaluation of the power producible at the turbine inlet linked to the water flow. The pipes and turbines were not integrated because they did not have an experimental device. It is in this context that a perfect fluid hypothesis is considered for water with pipe and turbine devices not causing energy losses. Losses are not ignored; the study is just restricted to the power producible at the turbine inlet.

From Eq. (6) for the determination of the wind turbine power at different altitudes which is the equivalent of the pumped storage power and Eq. (3) for the determination of the flow rate; implemented in ArcGIS and Matlab/Simulink software, the operation of the pumped storage system could be simulated. The first results are thus based on the flow rate, the available power, the reservoir capacity and the turbined volume per kilowatt-hour of energy produced.

Figure 7 shows the flow rate and turbine power as a function of the elevation.

The three-dimensional curve suggests a linear correlation between elevation, power, and flow rate. The higher the elevation, the greater the available power, and consequently the flow rate. This simulation predicts a production capacity ranging from 4 MW to 24 MW. The flow rate from the upper reservoir to the lower reservoir varies from 2 L/s to 13 L/s for wind turbines located at altitudes ranging from 200 m to 2300 m.

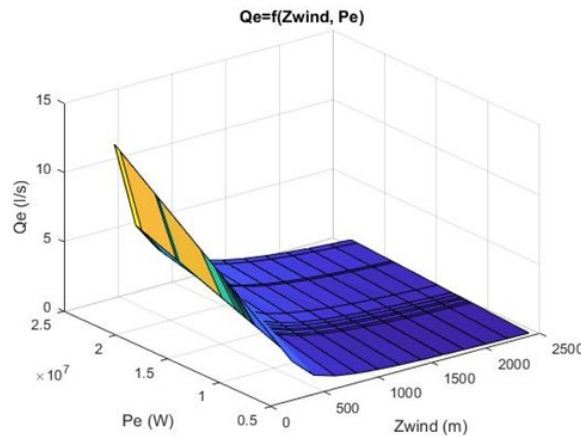


Figure 7. Flow rate and power available depending on the coast

4.3 Determination of Available Volume Based on the Coast

The study focused on assessing wind potential, evaluating the power output generated by water flow from one elevation to another, and studying the site's topography.

Any wind turbine with operating wind speeds within the Weibull distribution margin, with power output within the range of power output generated by water flow, and capable of being installed in a terrain with steep gradients, as it is the case in the study area, is suitable and can be operated. Figure 8, representing the two-dimensional curve of the volume of water turbined per kilowatt hour of energy produced, shows an exponential decrease as a function of the coast. This means that the capacity of the reservoir required to produce useful flow to supply our system is inversely proportional to the height. Basically, for coasts ranging from 200 m to 2300 m of altitude, volumes of water required ranging from 170 m^3 to 10 m^3 are obtained. To be more explicit, the capacity of the upstream lake is all the greater as the coast is low and vice versa when the coast is high.

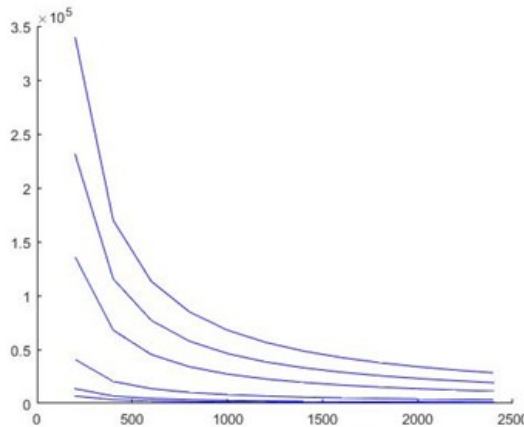


Figure 8. Water volume curve as a function of the level

4.4 Average Available Power of the Wind-PSP System

For hydraulic calculations, viscosity and turbulence effects are not taken into account because the hypothesis of water as a perfect fluid is considered, in addition, pipes and turbines are considered to operate without energy losses (idealized environment). These factors therefore have no effect on the calculation results.

Figure 9 shows the Red Cross as the curve representing the average power to be generated, i.e., a sort of median for useful energy production. This curve suggests useful reservoir capacities of around 10 m^3 to 95 m^3 of water for elevations ranging from 200 m to 2300 m. For production ranging from 4 MW to 24 MW, the equilibrium curve, which ensures an average production of around 12 MW, also follows an exponential decline as a function of elevation.

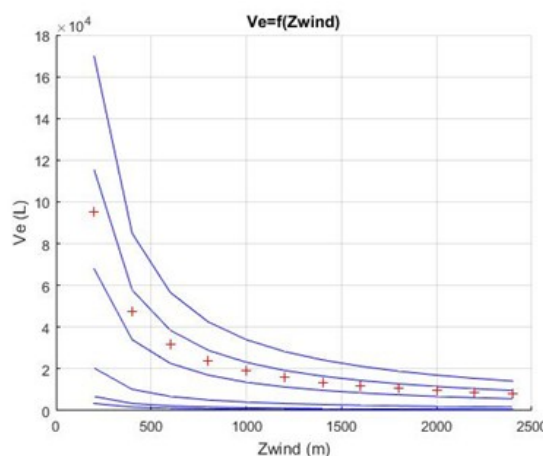


Figure 9. Average available power curve

The average turbine power obtained in this work, namely 12 MW, is almost 1000 times higher than that obtained by Rossi and al, namely 19.18 kW [11] (refer to Table 2). This large gap can be explained by the fact that in Rossi's work,

pump-turbine technology (PAT) is used for very small hydraulic or energy recovery applications. These machine tools are adapted in water distribution networks to adjust pressure levels and produce electricity. This gap could also be explained by the difference in topography between the two PSP sites and by the difference in energy source, which is the wind turbine in the context of this work.

Table 2. Main characteristics of the pump-turbine system operating in turbine mode at the BEP (best efficiency point) [11]

Parameter	Value
Flow rate value at the best efficiency point	152 m ³ /h
Liquid treated	H ₂ O ($\rho = 1000 \text{ kg/m}^3$)
Power	19.18 kW

4.5 Experimental Determination of River Flow in the Study Area

The float method incorporates the error and uncertainty of the method itself, due to which a correction coefficient is applied. The measurement results were verified three times and recorded in Table 3.

The marker extended 13 m along the watercourse. The measurement of the average depth of the watercourse gave $P = 1 \text{ m}$ (low water period) and could reach 2 m (flood period). The three bottles used covered the distance of 13 m with respective times $T_1 = 7S\ 53$; $T_2 = 7S\ 87$; $T_3 = 7S\ 11$. The measurement of the width of the bed being $W = 4.25 \text{ m}$. Deduction made from Eqs (23), (24) and (25):

Table 3. River flow rate (F) as a function of surface velocity (V_s), mean time (t), mean velocity (V_m), width (w) and mean depth (P_m)

L (m)	t (s)	V _s (m/s)	V _m (m/s)	W (m)	P _m (m)	Q (m ³ /s)
13	22.51	1.73	1.04	4.25	1	4.42

Comparison with the Literature

Compared with other studies, this river, with a flow rate of $15\ 912 \text{ m}^3/\text{h}$, flows 100 times faster than the flow rate in the work of Trenberth [8], or $152 \text{ m}^3/\text{h}$, capable of running turbines 100 times more efficient than the one used in this article. As mentioned previously, the difference between the results of these two studies stems from the topographic differences between the sites and the choice of application, which is very small-scale hydropower for Rossi and small-scale hydropower for the research. The difference in topographic profiles between the sites, as well as the storage capacities, may also explain the different observed differences. This comparison seems relevant for effectively sizing pipelines and turbines and estimating investment costs.

5 Conclusion

The proposed work consisted to model a renewable energy storage solution and evaluate its efficiency in an energy system powered mainly by intermittent renewable sources such as wind power in the context of Cameroon. The research explored gravity-based water storage through pumped-storage power stations (wind-PSP).

To achieve this, a set of mathematical and statistical models was implemented, including the Weibull distribution. This Weibull distribution used the collected annual meteorological data, extrapolated them, and established the Weibull fitting law.

The wind turbine power, Bernoulli flow model and simulation in dedicated applications assessed the flow rate, required water capacity, power output, and available energy quantities in the study area. In the study area (Nkongsamba, Cameroon), an average energy potential of 12 MWh for the wind power-PSP system was estimated for two water reservoirs with capacities of 95 m^3 and 10 m^3 , located at altitudes of 200 m and 2300 m respectively.

The experimental determination of the river's flow rate in the study area, estimated at $4.42 \text{ m}^3/\text{s}$, supports the hypothesis of efficient operation of a PSP. Similar work on pump-turbines for energy recovery applications, particularly a case study of an aqueduct (a canal intended to capture and conduct water from one place to another), evaluated an operating flow rate of $0.042 \text{ m}^3/\text{s}$.

For perspectives, a detailed assessment of Cameroon's water resources can be developed, leading to a risk assessment of overexploitation of this resource in the event of a wind power-PSP project; part integrated in an environmental and social impact study (ESIS).

An environmental and social management plan for the wind-PSP project could be considered; part integrated in an ESIS.

As perspective, an ESIS of the wind-PSP system could be considered. This study could integrate the calculations of reduction of GHG emissions.

An ESIS could be considered, a study which should include surveys on the social acceptance of the project and the support of the local community.

The impact of climate change could be considered in the ESIS of the wind-PSP project. The flexibility of the model could be determined by experimenting with the model under various operating conditions.

Technical analysis of the wind-PSP system could be considered and lead to the impacts of the system's productivity in the long term.

A techno-economic study of the wind-PSP system could be considered integrating the economic indicators and the cash flows of the project.

A study of wind turbine models on the performance of the wind-PSP system could be considered with the integration of the selection criteria.

As perspective, a technical-economic study of the wind-PSP system could be considered, leading to a maintenance and renovation plan.

A comparative study of the wind-PSP system with other energy storage technologies (such as battery storage) could be considered. In this study, the competitiveness of the model and the application scenarios could be deduced.

The comparison of the Weibull model with other models such as Rayleigh's could be considered in perspective.

An ESIS of the wind-PSP project can be considered; a study which will take into account the impacts of the project on the environment and local residents.

Data Availability

The data used to support the research findings are available from the corresponding author upon request.

Conflicts of Interest

The authors declare that they have no conflicts of interest.

References

- [1] N. Khan, Z. Shahid, M. M. Alam, A. A. B. Sajak, M. S. Mazlham, T. A. Khan, and S. S. A. Rizvi, "Energy management systems using smart grids: An exhaustive parametric comprehensive analysis of existing trends, significance, opportunities, and challenges," *Int. Trans. Electr. Energy Syst.*, vol. 2, pp. 1–38, 2022. <https://doi.org/10.1155/2022/3358795>
- [2] M. Farghali, A. I. Osman, Z. Chen, A. Abdelhaleem, I. Ihara, I. M. A. Mohamed, P. S. Yap, and D. W. Rooney, "Social, environmental, and economic consequences of integrating renewable energies in the electricity sector: A review," *Environ. Chem. Lett.*, vol. 21, no. 3, pp. 1381–1418, 2023. <https://doi.org/10.1007/s10311-023-01587-1>
- [3] D. Raimi, E. Campbell, R. G. Newell, B. Prest, S. Villanueva, and J. Wingenroth, "Global energy outlook 2022: Turning points and tension in the energy transition," *Resour. Future Wash.*, pp. 1723–1742, 2022. https://media.rff.org/documents/Report_22-04_v1.pdf
- [4] Y. W. Koholé, F. C. V. Fohagui, and G. Tchuen, "A holistic overview of Cameroon renewable energy sources: Potentials, achievements, challenges and perspectives," *Int. J. Ambient Energy*, vol. 43, no. 1, pp. 7308–7320, 2022. <https://doi.org/10.1080/01430750.2022.2068065>
- [5] A. Raouf, K. Njeudjang, J. G. T. Youmbi, X. Lu, J. Yue, E. C. Okoro, E. C. Odii, and A. M. A. Wahab, "Factors influencing groundwater development and mitigation strategies in Adamawa region, Cameroon: A critical review," *Sustain. Water Resour. Manag.*, vol. 11, no. 1, p. 5, 2025.
- [6] B. V. Bot, J. G. Tamba, and O. T. Sosso, "Assessment of biomass briquette energy potential from agricultural residues in Cameroon," *Biomass Convers. Biorefinery*, vol. 14, no. 2, pp. 1905–1917, 2024. <https://doi.org/10.1007/s13399-022-02388-2>
- [7] N. I. Zama, F. Lan, E. F. Zama, Y. Baninla, A. Millimouno, and Y. Yang, "Drivers of the water–energy–food nexus in Cameroon and implications for sustainable development," *Discov. Sustain.*, vol. 6, no. 1, p. 876, 2025. <https://doi.org/10.1007/s43621-025-01671-2>
- [8] K. E. Trenberth, "Climate change caused by human activities is happening and it already has major consequences," *J. Energy Nat. Resour. Law*, vol. 36, no. 4, pp. 463–481, 2018.
- [9] V. S. Limaye, "Making the climate crisis personal through a focus on human health," *Clim. Change*, vol. 166, no. 3, p. 43, 2021.
- [10] S. Kais and M. B. Mbarek, "Dynamic relationship between CO₂ emissions, energy consumption and economic growth in three North African countries," *Int. J. Sustain. Energy*, vol. 36, no. 9, pp. 840–854, 2017.
- [11] M. Rossi, M. Righetti, and M. Renzi, "Pump-as-Turbine for energy recovery applications: The case study of an aqueduct," *Energy Procedia*, vol. 101, pp. 1207–1214, 2016. <https://doi.org/10.1016/j.egypro.2016.11.163>
- [12] Z. Şen, "Reservoirs for water supply under climate change impact—A review," *Water Resour. Manag.*, vol. 35, no. 11, pp. 3827–3843, 2021. <https://doi.org/10.1007/s11269-021-02925-0>

- [13] N. Djongyang, R. Tchinda, and D. Djomo, “Estimation of some comfort parameters for sleeping environments in dry-tropical sub-Saharan Africa region,” *Energy Convers. Manage.*, vol. 58, pp. 110–119, 2012. <https://doi.org/10.1016/j.enconman.2012.01.012>
- [14] B. A. M. Nouadje, E. Kelly, R. H. T. Djielo, P. T. Kaben, G. Tchuen, and R. Tchinda, “Chad’s wind energy potential: An assessment of Weibull parameters using thirteen numerical methods for a sustainable development,” *Int. J. Ambient Energy*, vol. 45, no. 1, p. 2276119, 2024.
- [15] R. Tchinda and E. Kaptouom, “Wind energy in Adamawa and North Cameroon provinces,” *Energy Convers. Manage.*, vol. 44, no. 6, pp. 845–857, 2016.
- [16] E. M. Nfah and J. M. Ngundam, “Identification of stakeholders for sustainable renewable energy applications in Cameroon,” *Renew. Sustain. Energy Rev.*, vol. 16, no. 7, pp. 4661–4666, 2015. <https://doi.org/10.1016/j.rser.2012.05.019>
- [17] N. A. Arreyndip, E. Joseph, and A. David, “Wind energy potential assessment of Cameroon’s coastal regions for the installation of an onshore wind farm,” *Heliyon*, vol. 2, no. 11, p. e00187, 2016. <https://doi.org/10.1016/j.heliyon.2016.e00187>
- [18] F. H. Abanda, “Renewable energy sources in Cameroon: Potentials, benefits and enabling environment,” *Renew. Sustain. Energy Rev.*, vol. 16, no. 7, pp. 4557–4562, 2012. <https://doi.org/10.1016/j.rser.2012.04.011>
- [19] D. K. Kaoga, R. Danwe, S. Y. Doka, and N. Djongyang, “Statistical analysis of wind speed distribution based on sixWeibull Methods for wind power evaluation in Garoua, Cameroon,” *J. Renew. Energ.*, vol. 18, no. 1, pp. 105–125, 2015.
- [20] C. Kenfack-Sadem, R. Tagne, F. B. Pelap, and G. Nfor Bawe, “Potential of wind energy in Cameroon based on Weibull, normal, and lognormal distribution,” *Int. J. Energy Environ. Eng.*, vol. 12, no. 4, pp. 761–786, 2021. <https://doi.org/10.1007/s40095-021-00402-3>
- [21] D. K. Kaoga, N. Djongyang, S. Y. Doka, and D. Raidandi, “Assessment of wind energy potential for small scale water pumping systems in the north region of Cameroon,” *Int. J. Basic Appl. Sci.*, vol. 3, no. 1, pp. 38–46, 2014. <https://doi.org/10.14419/ijbas.v3i1.1769>
- [22] B. S. Pali and S. Vadhera, “A novel solar photovoltaic system with pumped-water storage for continuous power at constant voltage,” *Energy Convers. Manage.*, vol. 181, pp. 133–142, 2019. <https://doi.org/10.1016/j.enconman.2018.12.004>
- [23] A. G. Olabi, “Renewable energy and energy storage systems,” *Energy*, vol. 136, pp. 1–6, 2017. <https://doi.org/10.1016/j.energy.2017.07.054>
- [24] A. Schlie, D. Wille, S. Schulze, L. G. W. A. Cleophas, and I. Schaefer, “Detecting variability in MATLAB/Simulink models: An industry-inspired technique and its evaluation,” in *Proceedings of the 21st International Systems and Software Product Line Conference (SPLC’17)*, New York, NY, USA, 2017, pp. 215–224. <https://doi.org/10.1145/3106195.3106225>
- [25] D. K. Chaturvedi, *Modeling and Simulation of Systems using MATLAB and Simulink*. CRC Press, 2010.
- [26] M. Semenova, A. Vasileva, G. Lukina, and U. Popova, “Solving differential equations by means of mathematical simulation in Simulink spp of Matlab software package,” *Technol. Adv. Constr.*, vol. 180, pp. 417–431, 2022. https://doi.org/10.1007/978-3-030-83917-8_38
- [27] H. Klee and R. Allen, *Simulation of Dynamic Systems with MATLAB® and Simulink®*. CRC Press, 2018.
- [28] M. Liu, Z. Wen, and H. Su, “A multipoint prediction model for the deformation of concrete dams considering climatic features of high-altitude regions,” *Eng. Struct.*, vol. 319, p. 118845, 2024.
- [29] A. Terekhov, N. Makarenko, A. Pak, and N. Abayev, “Using the digital elevation model (DEM) and coastlines for satellite monitoring of small reservoir filling,” *Cogent Eng.*, vol. 7, no. 1, p. 1853305, 2020. <https://doi.org/10.1080/23311916.2020.1853305>
- [30] A. O. Altunel, “Suitability of open-access elevation models for micro-scale watershed planning,” *Environ. Monit. Assess.*, vol. 190, no. 9, p. 512, 2018. <https://doi.org/10.1007/s10661-018-6890-1>
- [31] M. Karaman and E. Özelen, “Comparative assessment of remote sensing-based water dynamic in a dam lake using a combination of Sentinel-2 data and digital elevation model,” *Environ. Monit. Assess.*, vol. 194, no. 2, p. 92, 2022. <https://doi.org/10.1007/s10661-021-09703-w>
- [32] J. K. Thakur, S. K. Singh, and V. S. Ekanthalu, “Integrating remote sensing, geographic information systems and global positioning system techniques with hydrological modeling,” *Appl. Water Sci.*, vol. 7, no. 4, pp. 1595–1608, 2017. <https://doi.org/10.1007/s13201-016-0384-5>
- [33] B. Ingleby, “Global assimilation of air temperature, humidity, wind and pressure from surface stations,” *Q. J. R. Meteorol. Soc.*, vol. 141, no. 687, pp. 504–517, 2015.
- [34] A. P. Selvam and S. N. S. Al-Humairi, “Environmental impact evaluation using smart real-time weather monitoring systems: A systematic review,” *Innov. Infrastruct. Solut.*, vol. 10, no. 1, p. 13, 2025.

- [35] R. Tateyama, E. Ohtani, H. Terasaki, K. Nishida, Y. Shibasaki, A. Suzuki, and T. Kikegawa, “Density measurements of liquid Fe–Si alloys at high pressure using the sink–float method,” *Phys. Chem. Miner.*, vol. 38, no. 10, pp. 801–807, 2011. <https://doi.org/10.1007/s00269-011-0452-1>
- [36] M. Y. Zakaria, D. A. Pereira, and M. R. Hajj, “Experimental investigation and performance modeling of centimeter-scale micro-wind turbine energy harvesters,” *J. Wind Eng. Ind. Aerodyn.*, vol. 147, pp. 58–65, 2015.
- [37] F. Xu, F. G. Yuan, L. Liu, J. Hu, and Y. Qiu, “Performance prediction and demonstration of a miniature horizontal axis wind turbine,” *J. Energy Eng.*, vol. 139, no. 3, pp. 143–152, 2013.
- [38] T. Kousksou, P. Bruel, A. Jamil, T. E. Rhafiki, and Y. Zeraouli, “Energy storage: Applications and challenges,” *Sol. Energy Mater. Sol. Cells*, vol. 120, pp. 59–80, 2014.
- [39] E. S. Akyüz, E. Telli, and M. Farsak, “Hydrogen generation electrolyzers: Paving the way for sustainable energy,” *Int. J. Hydrogen Energy*, vol. 81, pp. 1338–1362, 2024.
- [40] J. Dai, D. Liu, L. Wen, and X. Long, “Research on power coefficient of wind turbines based on SCADA data,” *Renew. Energy*, vol. 86, pp. 206–215, 2016.
- [41] M. Teimouri, S. M. Hoseini, and S. Nadarajah, “Comparison of estimation methods for the Weibull distribution,” *Statistics*, vol. 47, no. 1, pp. 93–109, 2013.

Nomenclature

P_1, P_2	Pressures, Pa
V_1, V_2	Velocities, m/s
h_1, h_2	Elevations, m
ρ	Density of water, kg/m ³
g	Acceleration due to gravity, ms ⁻²
Δh	Pressure drop, N/m ²
k	Coefficient
h	Head, m
F	Flow rate, m ³ / s
η	Turbine efficiency
P	Output power, W
V_{wind}	Wind speed, m/s
Z_{wind}	Height, m
$V_{\text{wind,ref}}$	Reference wind speed, m/s
$Z_{\text{wind,ref}}$	Reference height, m
z_0	Terrain roughness
P_{wind}	Wind power, W
ρ_a	Air density, kg/m ³
k, c, α	Coefficient
n	Number of non-zero data values
i	Measurement interval
v	Wind speed measured at interval i
V_s	Surface velocity, m/s
t	Mean time, s
V_m	Mean velocity, m/s
W	Width, m
P_m	Mean depth, m